

Review

# Non-Equilibrium Uranium as an Indicator of Global Climate Variations—The World Ocean and Large Lakes

Igor Tokarev<sup>1</sup> and Evgeny Yakovlev<sup>2,\*</sup><sup>1</sup> Research Park, St. Petersburg State University, 199155 St. Petersburg, Russia; tokarevigor@gmail.com<sup>2</sup> N. Laverov Federal Center for Integrated Arctic Research of UB RAS, 163000 Arkhangelsk, Russia

\* Correspondence: evgeny.yakovlev@fciarctic.ru; Tel.: +7-8182-21-15-71

**Abstract:** In natural water, as a rule, there is a violation of radioactive equilibrium in the chain  $^{238}\text{U} \dots \rightarrow ^{234}\text{U} \rightarrow ^{230}\text{Th} \rightarrow$ . Groundwater usually has a  $^{234}\text{U}/^{238}\text{U}$  ratio in the range of 0.8–3.0 (by activity). However, in some regions, the  $^{234}\text{U}/^{238}\text{U}$  ratio reaches >10 and up to 50. Ultrahigh excesses of  $^{234}\text{U}$  can be explained by climatic variations. During a cold period, minerals accumulate  $^{234}\text{U}$  as a normal component of the radioactive chain, and after the melting of permafrost, it is lost from the mineral lattice faster than  $^{238}\text{U}$  due to its higher geochemical mobility. This hypothesis was tested using data on the isotopic composition of uranium in the chemo- and bio-genic formations of the World Ocean and large lakes, which are reservoirs that accumulate continental runoff. The World Ocean has the most significant  $^{234}\text{U}$  enrichments in the polar and inland seas during periods of climatic warming in the Late Pleistocene and Holocene. In the bottom sediments of Lake Baikal, the  $^{234}\text{U}/^{238}\text{U}$  ratio also increases during warm periods and significantly exceeds the  $^{234}\text{U}$  excess of the World Ocean. Furthermore, the  $^{234}\text{U}/^{238}\text{U}$  ratio in the water of Lake Baikal and its tributaries increases from north to south following a decrease in the area of the continuous permafrost and has a seasonal variation with a maximum  $^{234}\text{U}/^{238}\text{U}$  ratio in summer. The behavior of  $^{234}\text{U}$  in large water reservoirs is consistent with the hypothesis about the decisive influence of permafrost degradation on the anomalies in  $^{234}\text{U}/^{238}\text{U}$  ratios in groundwater.

**Keywords:** non-equilibrium uranium;  $^{234}\text{U}/^{238}\text{U}$  ratio; climate variations; permafrost; World Ocean; Lake Baikal



**Citation:** Tokarev, I.; Yakovlev, E. Non-Equilibrium Uranium as an Indicator of Global Climate Variations—The World Ocean and Large Lakes. *Water* **2021**, *13*, 3514. <https://doi.org/10.3390/w13243514>

Academic Editor: Elias Dimitriou

Received: 5 November 2021

Accepted: 6 December 2021

Published: 9 December 2021

**Publisher's Note:** MDPI stays neutral with regard to jurisdictional claims in published maps and institutional affiliations.



**Copyright:** © 2021 by the authors. Licensee MDPI, Basel, Switzerland. This article is an open access article distributed under the terms and conditions of the Creative Commons Attribution (CC BY) license (<https://creativecommons.org/licenses/by/4.0/>).

## 1. Introduction

The violation of the radioactive equilibrium of the  $^{238}\text{U}$  chain ( $^{238}\text{U} \rightarrow ^{234}\text{Th} \dots ^{234}\text{U} \rightarrow ^{230}\text{Th} \rightarrow \dots ^{206}\text{Pb}$ , hereafter referred to as the  $^{234}\text{U}/^{238}\text{U}$  activity ratio) in natural water was discovered by P.I. Chalov [1–3] and V.V. Cherdyntsev [4,5]. They explained it by radio-kinetic separation, i.e., an increase in the mobility of daughter products in comparison with parent isotopes. For the majority of groundwater, the  $^{234}\text{U}/^{238}\text{U}$  ratio is in the range of 0.8–3 (hereafter, the activity ratio). Sometimes, in groundwater at middle and high latitudes of the Earth, there is a steady shift of the  $^{234}\text{U}/^{238}\text{U}$  ratio to 5–20, and in some cases, it increases to 50 [6,7]. Such high enrichment in uranium-234 is explained by the release of recoil atoms ( $^{234}\text{Th}$ ) from the mineral matrix into the water [8–16]. A limitation of this hypothesis is the fact that significant enrichment in uranium-234 can occur only with a high dispersion of the mineral grains, with characteristic radii  $r < 10^{-5}$  m and with water–rock interaction lasting a relatively long time ( $t > 10^4$  years).

V.A. Polyakov [6] suggested that extremely high excesses of uranium-234 could be related to climatic variations. During a cold period, due to the absence of liquid water,  $^{234}\text{U}$  accumulates in host rocks as a normal component of the  $^{238}\text{U}$  chain. After permafrost degradation, uranium-234 is extracted from the host rocks by meltwater at a higher rate than  $^{238}\text{U}$ , since  $^{234}\text{U}$  has a predominantly water-soluble form  $\text{U}^{6+}$  and is located in the conjugated tracks of recoil nuclei and  $\alpha$ -particles. In contrast,  $^{238}\text{U}$  has a water-insoluble form  $\text{U}^{4+}$  as the chemical component of its mineral lattice. As a result, according to

our estimates, the bulk diffusion coefficient of uranium-234 in minerals exceeds that for uranium-238 by approximately 500 times.

This hypothetical mechanism received confirmation from a complex study of groundwater, including the determination of  $\delta^{18}\text{O}$ ,  $\delta^2\text{H}$ , and  $^{234}\text{U}/^{238}\text{U}$  and the dating of groundwater by the helium technique [17–21]. A more fundamental test of the hypothesis is possible on the basis of data on the isotopic composition of uranium in chemo- and biogenic formations in the World Ocean and large continental water bodies.

## 2. World Ocean

The average ( $^{234}\text{U}/^{238}\text{U}$ ) ratio for the modern ocean is 1.144–1.145 [22,23], and the weighted mean for river runoff is 1.25 [24]. If rivers are the only source of  $^{234}\text{U}$ , then, taking into account the average residence time of U in the oceans of ~400 thousand years [9,25], the  $^{234}\text{U}/^{238}\text{U}$  ratio in ocean water should be ~1.08 [22,26,27]. This difference in the calculated and observed  $^{234}\text{U}/^{238}\text{U}$  ratios in ocean water cannot be explained by variations in river runoff and/or a decrease in the residence time of uranium in the ocean [28]. Therefore, there must be an additional source of uranium-234.

Hypothetically, it could be  $^{234}\text{Th}$  nuclei, which directly recoil from the mineral lattice to water. If recoil  $^{234}\text{Th}$  is the main reason for the  $^{234}\text{U}/^{238}\text{U}$  disequilibrium, then  $^{234}\text{U}$  excess should correlate with the global increase in the physical disintegration of rocks during glacial periods [29–31]. An additional source of uranium-234 during a glaciation time should be clayey sediments on shelves, which drained after a drop in the ocean level and were accumulated in a previous warm period [32]. Following these hypotheses, which link the  $^{234}\text{U}$  excess with an increase in the flux of  $^{234}\text{Th}$  recoil nuclei, the highest value of  $^{234}\text{U}/^{238}\text{U}$  ratio in seawater should be observed during a glaciation time. As will be shown below, this contradicts the observations and, in addition, these hypotheses do not answer the following questions.

1. Why is the loss of  $^{234}\text{Th}$  recoil nuclei by fine-grained particles small at the continental stage of transport? In the zone of finely dispersed rocks on the continents, Yedoma (Arctic), loess, and black earth (middle latitudes), whose origin is associated with the wind spread of dusty material during the glacial epochs, a significant violation of the radioactive equilibrium in the  $^{238}\text{U}$  chain is not observed in surface and shallow groundwater.
2. Suppose that the increase in the amount of  $^{234}\text{Th}$  recoil nuclei is, in fact, due to an increase in the supply of dust to the ocean during cooling periods [33,34]. However, both dust and thorium in the chemical compounds have a very short average residence time in ocean water [35–37] and are quickly deposited in bottom sediments. What mechanism ensures the reverse flow of uranium from the pore water of sediments into ocean water? Oxidizing conditions favoring the migration of uranium in water-soluble forms are observed only in the thin surface layer of bottom sediments. The presence of organic material, for example, in the form of microbial mats and/or a stream of dead organisms, transforms the environmental conditions into an area of chemical reduction. The diffuse transfer of uranium from pore water into free water is hampered by the accumulation of new portions of sediments, with the exception of the oceanic abyssal, where the accumulation is greatly slowed down. In some cases, when an excess of uranium  $^{234}\text{U}$  ( $^{234}\text{U}/^{238}\text{U} > 1.14$ ) is observed in the pore water, occasionally, none is recorded for the abyssal [10,13–15].

The generalization of data on corals, mollusk valves, and carbonate marine sediments demonstrates a noticeable change of the  $^{234}\text{U}/^{238}\text{U}$  ratio in time, with a maximum during warming periods (Figure 1). The minimum of the uranium-234 excess in the ocean is observed during the last glaciation period.

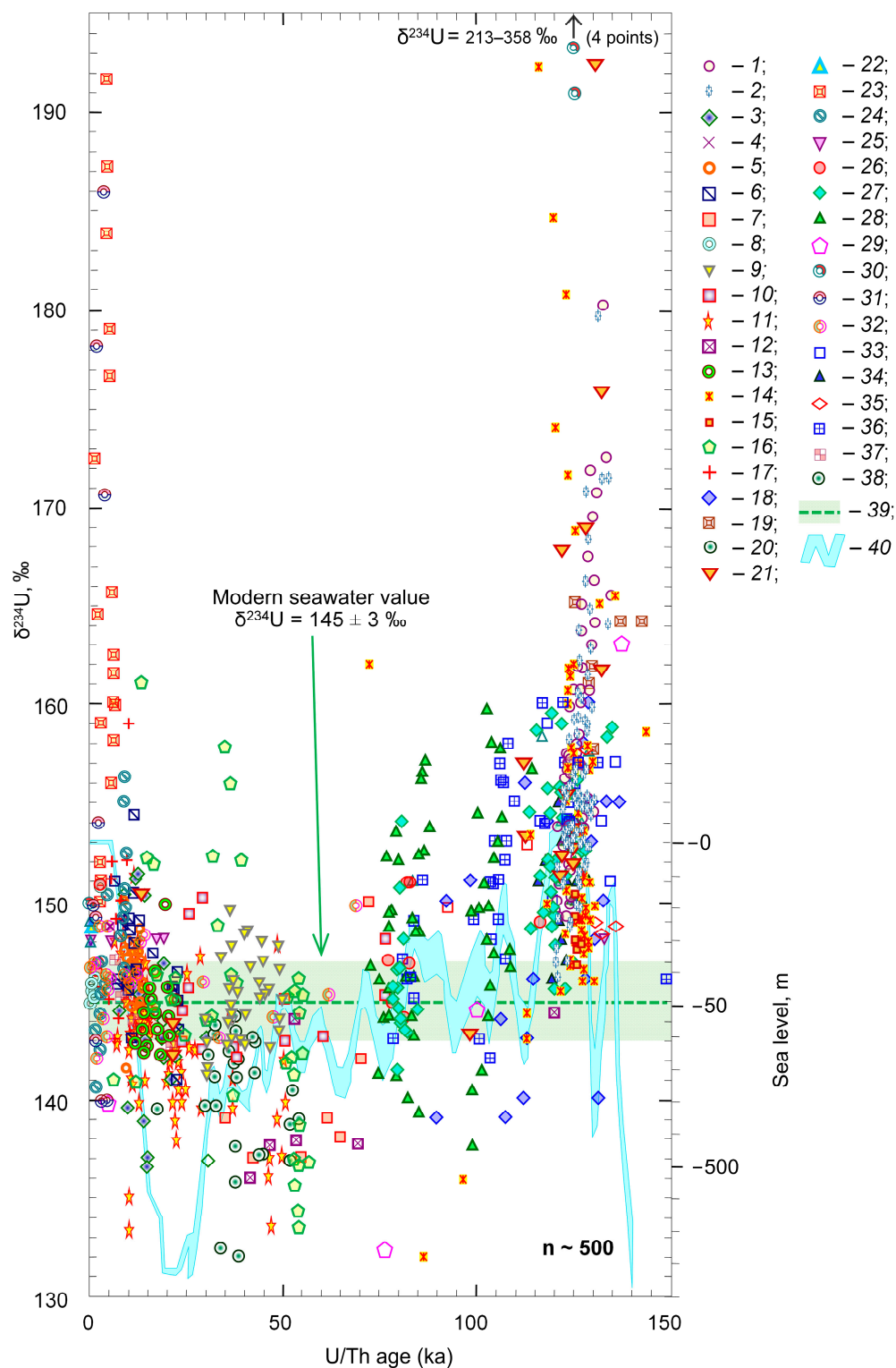


**Figure 1.** Initial uranium isotopic composition ( $^{234}\text{U}/^{238}\text{U}$ ) in corals and carbonates of the circumpolar and arctic regions of the World Ocean: 1—[38]; 2—[39]; 3—[40]; 4—[41]; 5—[42]; 6—[43]; 7—[44]; 8—[45]; 9—[46]; 10—[47]; 11—[48]; 12—[49]; 13—[50]; 14—[51]; 15—[52]; 16—[53]; 17—[54]; 18—[55]; 19—[32]; 20—[56]; 21—[57]; 22—[58]; 23—[59]; 24—[60]; 25—[61]; 26—[62]; 27—[63]; 28—[64]; 29—[65]; 30—[66]; 31—[67]; 32—[68]; 33—[69]; 34—[70]; 35—[71]; 36—[72]; 37—[73]; 38—[74]; 39—uranium isotopic composition in modern ocean  $\delta^{234}\text{U} = 145 \pm 3 \text{ ‰}$  [22,23]; 40—sea-level changes [75].

The observed distribution of the  $^{234}\text{U}/^{238}\text{U}$  ratio in time for oceanic chemo- and organogenic formations is much better explained by the hypothesis linking the increase in the uranium-234 flux with permafrost melting, which contradicts the hypothesis that

the increase in  $^{234}\text{U}$  excess is related to an increase in the flux of  $^{234}\text{Th}$  recoil nuclei. For the Eemian interglacial, which was warmer than the current one, the recorded excess of uranium-234 was somewhat higher than the Holocene excess, probably due to the greater degree of permafrost thawing. For the  $^{234}\text{U}/^{238}\text{U}$  ratio distribution curve during the Weichselian glaciation, a fine structure is found, when small increases in the  $^{234}\text{U}/^{238}\text{U}$  ratio correspond to periods of temporary warming within the cooling periods.

No significant excess of uranium-234 was found in the corals, shells of mollusks, and carbonate deposits of the equatorial ocean zone [23]. In contrast, the Arctic Ocean, being relatively isolated and experiencing the greatest influence of the continental runoff from the permafrost zone, demonstrates the maximum excesses of the  $^{234}\text{U}/^{238}\text{U}$  ratio. For example, in the Barents Sea, the uranium concentration is  $(0.49\text{--}35.6) \times 10^{-7}$  g/L, and the activity ratio varies from 1.11 to 1.91 [18–76]. Based on the flow patterns of the Barents Sea, the highest excess of uranium-234 is observed in areas with a minimal contribution of Atlantic water.

Following  $^{234}\text{U}$ , anomalies should also be found in the isotopic composition of thorium. Considering the time required to achieve radioactive equilibrium in the  $^{234}\text{U} \rightarrow ^{230}\text{Th} \rightarrow ^{226}\text{Ra} \dots$  chain, the anomalies in the  $^{230}\text{Th}/^{232}\text{Th}$  ratio caused by the influence of climatic variations should be traced much farther into the past than the  $^{234}\text{U}/^{238}\text{U}$  ratio. For example, in the Norwegian Sea, the Holocene, Eemian, and previous warming periods (MIS-1, MIS-5, and MIS-7, respectively, Figure 2) are unambiguously distinguished by an increase in excess thorium-230 and the depletion of the oxygen isotopic composition in carbonates.

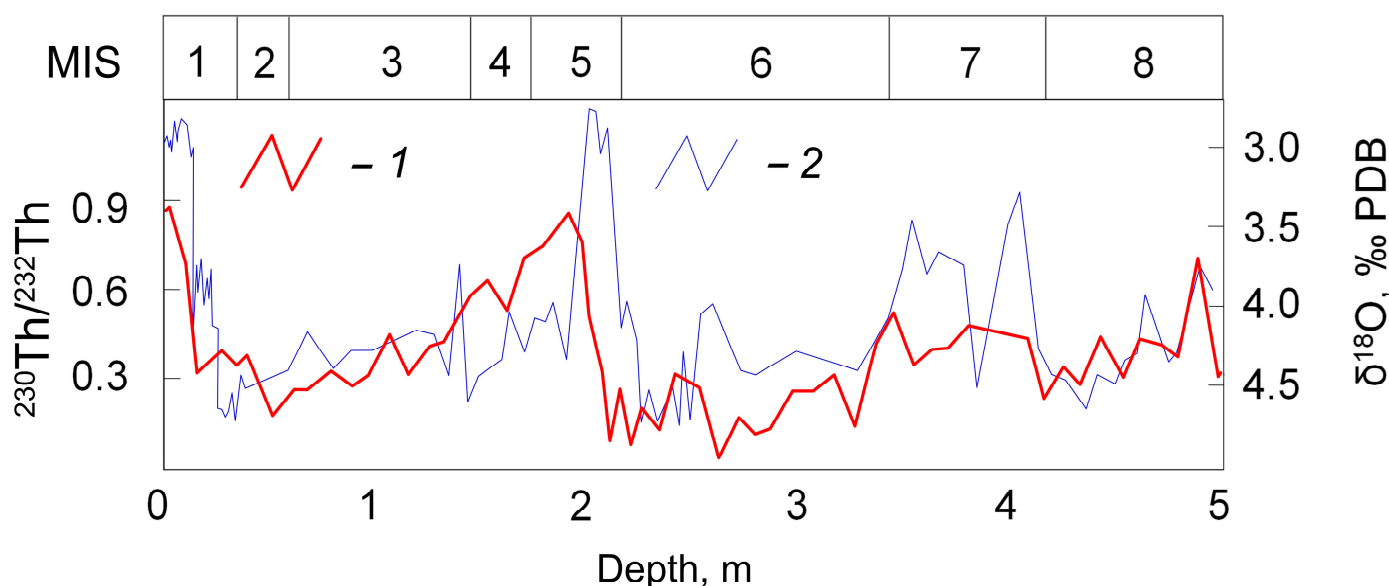


**Figure 2.** Initial  $^{230}\text{Th}/^{232}\text{Th}$  ratio and oxygen isotopic composition of carbonates for core 23059 from the Norwegian Sea for the period MIS 1–8 (adapted from [77] with changes): 1— isotopic composition of thorium; 2— isotopic composition of oxygen.

### 3. Continental Freshwater Bodies

Lake Baikal is the largest reservoir of freshwater, and it is located in a geographic zone where the temperature state of rocks in the Late Pleistocene and Holocene changed significantly [78]. The catchment area of Lake Baikal currently contains both sporadic discontinuous and continuous permafrost. The modern warming and thawing of the permafrost characteristic of the region [79] affect the volume and chemical composition of river runoff [80].

In the bottom sediments of Lake Baikal, geochemical, mineral, and biological systems react to climatic variations [81–108]. During warming, the concentration of diatoms sharply

increases, and in cold periods, the flow of clay material and the fraction of terrigenous uranium increases (Figure 3a).

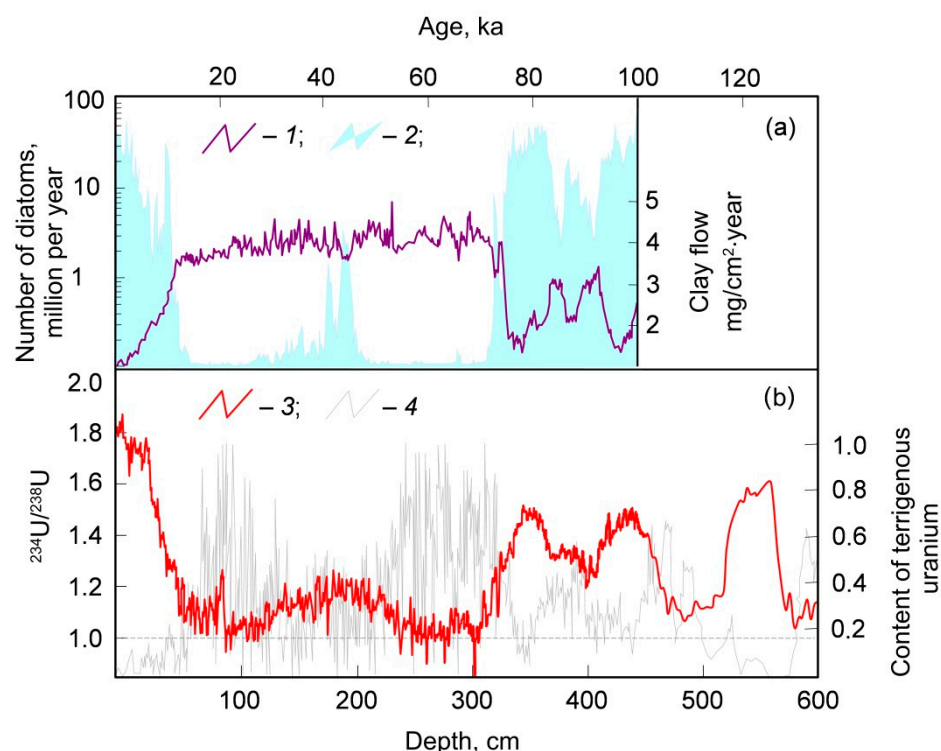


**Figure 3.** Distribution of various biological, clastic and isotope-geochemical indicators over the depth of bottom sediments of Lake Baikal (adapted with changes from [84,85]: 1—clay flow (a); 2—number of diatoms (a); 3— $^{234}\text{U}/^{238}\text{U}$  ratio (b); 4—concentration of terrigenous uranium (b).

The enrichment in uranium-234 significantly decreases in cold periods and increases in warm ones (Figure 3b). A decrease in the amount of uranium-234 during cold periods with a simultaneous increase in the flow of clay into the lake contradicts the hypothesis of the direct input of  $^{234}\text{Th}$  into the water as the main source of imbalance in the  $^{238}\text{U}$  system [8–16,109].

Similar variations in isotopic, geochemical, and biogenic parameters were found in the bottom sediments of some water bodies in northern and northwestern Mongolia, for example, Lake Huvsgul [110–119]. Vosel [120] studied the bottom sediments of the small lakes of the Baikal region. The highest enrichment in uranium-234 was found in the lakes Tsagan-Tyrm (the saltiest lake,  $^{234}\text{U}/^{238}\text{U} = 2.7$ —hereafter, on average), Melkoye ( $^{234}\text{U}/^{238}\text{U} = 2.6$ ), and Ordynskoye ( $^{234}\text{U}/^{238}\text{U} = 2.3$ ); lower enrichment was found in the lakes Holbo-Nur ( $^{234}\text{U}/^{238}\text{U} = 1.9$ ), Namshi-Nur (the least mineralized lake,  $^{234}\text{U}/^{238}\text{U} = 1.8$ ), and Alaty ( $^{234}\text{U}/^{238}\text{U} = 1.7$ ). There is a correlation between an increase in the  $^{234}\text{U}/^{238}\text{U}$  ratio and lake water salinity that can be explained by the accelerated degradation of permafrost upon contact with saltwater.

A network of tributaries is the source of uranium in the bottom sediments of Lake Baikal. Currently, in the Selenga River (south sector of the catchment), the  $^{234}\text{U}/^{238}\text{U}$  ratio is 2.08–2.13 (average 2.11); in the Upper Angara River (north sector of the catchment), it is  $1.34 \pm 0.02$  and  $1.40 \pm 0.15$  [84,90]. In the Barguzin River (middle sector of catchment), it is  $1.53 \pm 0.03$  and  $1.56 \pm 0.14$  [84,90]. In the Selenga River, seasonal variations were obtained, with a maximum of the  $^{234}\text{U}/^{238}\text{U}$  ratio in summer, as well as a decrease in this ratio from the source (mountain part of the watershed, Figure 4) to the mouth [84,121]. There is a stable differentiation between the southern and northern sectors of the Lake Baikal catchment by uranium-234 excess, with its maximum in the south in the zone of the most intense modern permafrost degradation.

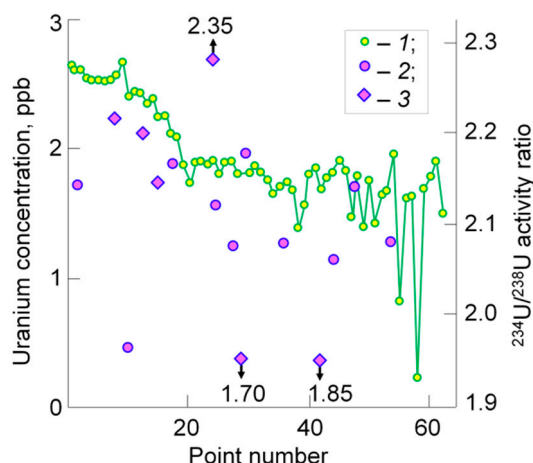


**Figure 4.** The content and isotopic composition of uranium in the Selenga River (the profile length is approximately 400 km, point 1 is on the border with Mongolia, and point 60 is at the mouth) and its tributaries (adapted from [84]): 1—uranium concentration in water of Selenga River; 2, 3—isotopic composition of uranium in water of Selenga River and its tributaries, respectively.

Apparently, the seasonal thawing of permafrost (Figure 5) affects the isotopic composition of uranium in surface and groundwater, leading to an increase in uranium-234 at the end of the warm season [122]. The depth of seasonal permafrost thawing depends on factors related to weather. Therefore, the seasonal enrichment by uranium-234 varies significantly from year to year.

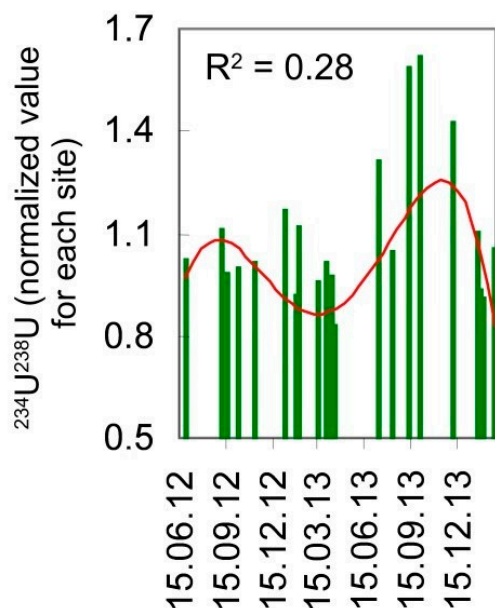


**Figure 5.** Change in the isotopic composition of uranium ( $^{234}\text{U}/^{238}\text{U}$ ) of surface (5 monitoring points) and groundwater (36 monitoring points) of the Kultuk test site, southern Baikal region (data from Table 1 after [122]): the  $^{234}\text{U}/^{238}\text{U}$  ratio is normalized to the average for each sampling point, and the curve is a polynomial of degree four, which gives the first best approximation in  $R^2$  (more reliable detection of seasonal variations is hindered by the uneven sampling of water in time).

#### 4. Conclusions

In the World Ocean, the most significant enrichments in uranium-234 and thorium-230 are recorded for the northern and inland seas during warming climate periods. The relative  $^{234}\text{U}$  enrichment is greater in places where (1) the sea is more isolated from the general oceanic circulation, (2) the relative length of the coastline is greater, and (3) the contribution of continental waters to the chemical balance of the water budget is greater. In

the bottom sediments of Lake Baikal during periods of cooling, the isotopic composition of uranium approaches the equilibrium value  $^{234}\text{U}/^{238}\text{U} = 1$ , and during periods of warming, the excess of uranium-234 increases even more significantly than in the oceanic reservoir. In the tributaries of Lake Baikal and small lakes on its catchment, an increase in excess uranium-234 is noted from north to south, in accordance with a decrease in the proportion of the area occupied by the continuous permafrost. Since the source of excess uranium-234 in the ocean and large lakes is runoff from the continents, the appearance of anomalously increased  $^{234}\text{U}/^{238}\text{U}$  ratios indicates permafrost melting. The revealed effect is consistent with the hypothesis according to which the accumulation of the radiogenic product  $^{234}\text{U}$  in the mineral matrix occurs during the ice age in the frozen rocks. In the course of permafrost degradation and ice melting, the flux of uranium-234 from the host rocks into the meltwater increases significantly due to its greater mobility as compared to uranium-238.

**Author Contributions:** All authors contributed to the study conception and design. Conceptualization, validation, and writing—original draft preparation were performed by I.T. Formal analysis and investigation were performed by I.T. and E.Y. Writing—review and editing were performed by I.T. Funding acquisition was performed by E.Y. Project administration and resources were performed by E.Y. and I.T. Supervision and visualization were performed by I.T. All authors have read and agreed to the published version of the manuscript.

**Funding:** The work was supported by the Russian Science Foundation grant No. 20-77-10057 “Diagnostics of permafrost degradation based on isotope tracers ( $^{234}\text{U}/^{238}\text{U}$ ,  $\delta^{18}\text{O} + \delta^2\text{H}$ ,  $\delta^{13}\text{C} + ^{14}\text{C}$ ).

**Institutional Review Board Statement:** Not applicable.

**Informed Consent Statement:** Not applicable.

**Data Availability Statement:** The datasets presented in this study can be obtained upon request to the corresponding author.

**Conflicts of Interest:** The authors declare no conflict of interest.

## References

- Chalov, P.I. Study of U(II)/U(I) Ratios in Some Natural Objects. Ph.D. Thesis, Academy of Sciences of the KazakhSSR, Alma-Ata, USSR, 1954.
- Chalov, P.I. U234/U238 isotopic ratio in some secondary minerals. *Geochemistry* **1959**, *2*, 165–170.
- Chalov, P.I. *Isotopic Fractionation of Natural Uranium*; Ilim: Frunze, Russia, 1975.
- Cherdyntsev, V.V. *Uran-234*; Atomizdat: Moscow, Russia, 1967.
- Cherdyntsev, V.V. *Isotopic Composition of Radioelements in Natural Objects and Their Importance in Geochronology*; Institute of Precambrian Geology and Geochronology: Moscow, Russia, 1955.
- Polyakov, V.A. *Study of Changes in Hydrochemistry and Groundwater Resources of Coastal Water Intakes in Estonia from Isotope Data*; GIDEK: Zvenigorod, Russia, 1991.
- Arndt, M.F.; West, L. A Study of the Factors Affecting the Gross Alpha Measurement, and a Radiochemical Analysis of Some Groundwater Samples from the State of Wisconsin Exhibiting an Elevated Gross Alpha Activity. Wisconsin Groundwater Management Practice Monitoring Project, DNR-176. 2004. Available online: <https://wri.wisc.edu/wp-content/uploads/FinalWR02R009.pdf> (accessed on 1 November 2021).
- Ku, T.-L. An evaluation of the U234/U238 method as a tool for dating pelagic sediments. *J. Geophys. Res. Space Phys.* **1965**, *70*, 3457–3474. [[CrossRef](#)]
- Ku, T.-L.; Mathieu, G.G.; Knauss, K. Uranium in Open Ocean: Concentration and isotopic composition. *Deep. Sea Res.* **1977**, *24*, 1005–1017. [[CrossRef](#)]
- Cochran, J.K.; Krishnaswami, S. Radium, thorium, uranium, and  $^{210}\text{Pb}$  in deep-sea sediments and sediment pore waters from the North Equatorial Pacific. *Am. J. Sci.* **1980**, *280*, 849–889. [[CrossRef](#)]
- Ivanovich, M.; Harmon, R.S. *Uranium-Series Disequilibrium*; Clarendon Press: Oxford, UK, 1992.
- Russell, A.D.; Edwards, R.L.; Hoff, J.A.; McCorkle, D.; Sayles, F. Sediment source of  $^{234}\text{U}$  suggested by  $\text{d}^{234}\text{U}$  in North Pacific pore waters. *Fall Meet. Suppl. EOS* **1994**, *75*, 332.
- Russell, A.D.; Emerson, S.; Nelson, B.K.; Erez, J.; Lea, D.W. Uranium in foraminiferal calcite as a recorder of seawater uranium concentrations. *Geochim. Cosmochim. Acta* **1994**, *58*, 671–681. [[CrossRef](#)]
- Henderson, G.M.; Burton, K.W. Using ( $^{234}\text{U}/^{238}\text{U}$ ) to assess diffusion rates of isotope tracers in ferromanganese crusts. *Earth Planet. Sci. Lett.* **1999**, *170*, 169–179. [[CrossRef](#)]

15. Henderson, G.M.; Slowey, N.C.; Haddad, G.A. Fluid flow through carbonate platforms: Constraints from  $^{234}\text{U}/^{238}\text{U}$  and  $\text{Cl}^-$  in Bahamas pore-waters. *Earth Planet. Sci. Lett.* **1999**, *169*, 99–111. [[CrossRef](#)]
16. Calsteren, V.; Thomas, L. Uranium-series dating applications in natural environmental science. *Earth-Sci. Rev.* **2006**, *75*, 155–175. [[CrossRef](#)]
17. Tokarev, I.V. Using isotope data ( $\delta^2\text{H}$ ,  $\delta^{18}\text{O}$ ,  $^{234}\text{U}/^{238}\text{U}$ ) in studying the processes of permafrost degradation as a result of long-term climate variations. *J. Min. Inst.* **2008**, *176*, 191–195.
18. Tokarev, I.V. Non-equilibrium uranium ( $^{234}\text{U}/^{238}\text{U}$ ) of water bodies and climatic variations. 1. Oceanic reservoir. *Geochem. Int.* **2021**, in press.
19. Tokarev, I.V.; Zubkov, A.A.; Rumynin, V.G.; Polyakov, V.A.; Kuznetsov VYu Maksimov, F.E. Origin of high  $^{234}\text{U}/^{238}\text{U}$  ratio in post-permafrost aquifers. In *Uranium in the Environment (Mining Impact and Consequences)*; Merkel, B.J., Hasche-Berger, A., Eds.; Taylor & Francis: London, UK, 2006; pp. 847–856.
20. Tokarev, I.; Zubkov, A.A.; Rumynin, V.G.; Pozdnyakov, S.P.; Polyakov, V.A.; Kuznetsov, V.Y. Assessment of the long-term safety of radioactive waste disposal: 1. Paleoreconstruction of groundwater formation conditions. *Water Resour.* **2009**, *36*, 206–213. [[CrossRef](#)]
21. Tokarev, I.; Zubkov, A.A.; Rumynin, V.G.; Pozdnyakov, S.P. Assessment of the long-term safety of radioactive waste disposal: 2. Isotopic study of water exchange in a multilayer system. *Water Resour.* **2009**, *36*, 345–356. [[CrossRef](#)]
22. Chen, J.H.; Edwards, R.L.; Wasserburg, G.J.  $^{238}\text{U}$ ,  $^{234}\text{U}$  and  $^{232}\text{Th}$  in seawater. *Earth Planet. Sci. Lett.* **1986**, *80*, 241–251. [[CrossRef](#)]
23. Henderson, G.M.; Anderson, R.F. The U-series toolbox for paleoceanography. *Rev. Mineral. Geochem.* **2003**, *52*, 493–532. [[CrossRef](#)]
24. Chabaux, F.; Riotte, J.; Dequincey, O. U-Th-Ra Fractionation during Weathering and River Transport. *Rev. Miner. Geochem.* **2003**, *52*, 533–576. [[CrossRef](#)]
25. Dunk, R.; Mills, R.; Jenkins, W. A reevaluation of the oceanic uranium budget for the Holocene. *Chem. Geol.* **2002**, *190*, 45–67. [[CrossRef](#)]
26. Cheng, H.; Adkins, J.; Edwards, R.; Boyle, E.A. U-Th dating of deep-sea corals. *Geochim. Cosmochim. Acta* **2000**, *64*, 2401–2416. [[CrossRef](#)]
27. Robinson, L.F.; Belshaw, N.S.; Henderson, G.M. U and Th isotopes in seawater and modern carbonates from the Bahamas. *Geochim. Cosmochim. Acta* **2004**, *68*, 1777–1789. [[CrossRef](#)]
28. Henderson, G.M. Seawater ( $^{234}\text{U}/^{238}\text{U}$ ) during the last 800 thousand years. *Earth Planet. Sci. Lett.* **2002**, *199*, 97–110. [[CrossRef](#)]
29. Kronfeld, J.; Vogel, J. Uranium isotopes in surface waters from southern Africa. *Earth Planet. Sci. Lett.* **1991**, *105*, 191–195. [[CrossRef](#)]
30. Kronfeld, J. Uranium deposition and Th-234 alpha-recoil: An explanation for extreme U-234/U-238 fractionation within the trinity aquifer. *Earth Planet. Sci. Lett.* **1974**, *21*, 327–330. [[CrossRef](#)]
31. Kronfeld, J.; Gradsztajn, E.; Müller, H.; Radin, J.; Yaniv, A.; Zach, R. Excess  $^{234}\text{U}$ : An aging effect in confined waters. *Earth Planet. Sci. Lett.* **1975**, *27*, 342–345. [[CrossRef](#)]
32. Esat, T.M.; Yokoyama, Y. Correlated Uranium and Sea-Level Fluctuations in Late Quaternary Oceans. *J. Goldschmidt Conf. Abstr.* **2000**, *5*, 387–388.
33. Muhs, D.R. The geologic records of dust in the Quaternary. *Aeolian Res.* **2013**, *9*, 3–48. [[CrossRef](#)]
34. Rea, D.K. The paleoclimatic record provided by eolian deposition in the deep sea: The geologic history of wind. *Rev. Geophys.* **1994**, *32*, 159–195. [[CrossRef](#)]
35. Anderson, R.F.; Cheng, H.; Edwards, R.L.; Fleisher, M.Q.; Hayes, C.T.; Huang, K.-F.; Kadko, D.; Lam, P.J.; Landing, W.M.; Lao, Y.; et al. How well can we quantify dust deposition to the ocean? *Phil. Trans. R. Soc. A* **2016**, *374*, 20150285. [[CrossRef](#)] [[PubMed](#)]
36. Broecker, W.; Kaufman, A.; Trier, R. The residence time of thorium in surface sea water and its implications regarding the rate of reactive pollutants. *Earth Planet. Sci. Lett.* **1973**, *20*, 35–44. [[CrossRef](#)]
37. Moore, W.S. The thorium isotope content of ocean water. *Earth Planet. Sci. Lett.* **1981**, *53*, 419–426. [[CrossRef](#)]
38. Bar-Matthews, M.; Wasserburg, G.; Chen, J. Diagenesis of fossil coral skeletons: Correlation between trace elements, textures, and  $^{234}\text{U}/^{238}\text{U}$ . *Geochim. Cosmochim. Acta* **1993**, *57*, 257–276. [[CrossRef](#)]
39. Thompson, W.G.; Curran, H.A.; Wilson, M.A.; White, B. Sea-level oscillations during the last interglacial highstand recorded by Bahamas corals. *Nat. Geosci.* **2011**, *4*, 684–687. [[CrossRef](#)]
40. Bard, E.; Hamelin, B.; Fairbanks, R.G. U-Th ages obtained by mass spectrometry in corals from Barbados: Sea level during the past 130,000 years. *Nature* **1990**, *346*, 456–458. [[CrossRef](#)]
41. Bard, E.; Fairbanks, R.G.; Hamelin, B.; Zindler, A.; Hoang, C.T. Uranium-234 anomalies in corals older than 150,000 years. *Geochim. Cosmochim. Acta* **1991**, *55*, 2385–2390. [[CrossRef](#)]
42. Bard, E.; Hamelin, B.; Arnold, M.; Montaggioni, L.; Cabioch, G.; Faure, G.; Rougerie, F. Deglacial sea-level record from Tahiti corals and the timing of global meltwater discharge. *Nature* **1996**, *382*, 241–244. [[CrossRef](#)]
43. Cabioch, G.; Ayliffe, L.K. Raised Coral Terraces at Malakula, Vanuatu, Southwest Pacific, Indicate High Sea Level During Marine Isotope Stage 3. *Quat. Res.* **2001**, *56*, 357–365. [[CrossRef](#)]
44. Chappell, J.; Omura, A.; Esat, T.; McCulloch, M.; Pandolfi, J.; Ota, Y.; Pillans, B. Reconciliation of late Quaternary sea levels derived from coral terraces at Huon Peninsula with deep sea oxygen isotope records. *Earth Planet. Sci. Lett.* **1996**, *141*, 227–236. [[CrossRef](#)]

45. Copard, K.; Colin, C.; Henderson, G.; Scholten, J.; Douville, E.; Sicre, M.-A.; Frank, N. Late Holocene intermediate water variability in the northeastern Atlantic as recorded by deep-sea corals. *Earth Planet. Sci. Lett.* **2012**, *313–314*, 34–44. [[CrossRef](#)]
46. Chiu, T.; Fairbanks, R.G.; Mortlock, R.A.; Bloom, A.L. Extending the radiocarbon calibration beyond 26,000 years before present using fossil corals. *Quat. Sci. Rev.* **2005**, *24*, 1797–1808. [[CrossRef](#)]
47. Cutler, K.; Edwards, R.; Taylor, F.; Cheng, H.; Adkins, J.; Gallup, C.; Cutler, P.; Burr, G.; Bloom, A. Rapid sea-level fall and deep-ocean temperature change since the last interglacial period. *Earth Planet. Sci. Lett.* **2003**, *206*, 253–271. [[CrossRef](#)]
48. Cutler, K.B.; Gray, S.C.; Burr, G.S.; Edwards, R.L.; Taylor, F.W.; Cabioch, G.; Beck, J.W.; Cheng, H.; Moore, J. Radiocarbon Calibration and Comparison to 50 Kyr BP with Paired  $^{14}\text{C}$  and  $^{230}\text{Th}$  Dating of Corals from Vanuatu and Papua New Guinea. *Radiocarbon* **2004**, *46*, 1127–1160. [[CrossRef](#)]
49. Dia, A.N.; Cohen, A.S.; O’Nions, R.K.; Shackleton, N.J. Seawater Sr isotope variation over the past 300 kyr and influence of global climate cycles. *Nature* **1992**, *356*, 786–788. [[CrossRef](#)]
50. Douarin, M.; Elliot, M.; Noble, S.R.; Sinclair, D.; Henry, L.-A.; Long, D.; Moreton, S.G.; Roberts, J.M. Growth of north-east Atlantic cold-water coral reefs and mounds during the Holocene: A high resolution U-series and  $^{14}\text{C}$  chronology. *Earth Planet. Sci. Lett.* **2013**, *375*, 176–187. [[CrossRef](#)]
51. Dutton, A.; Webster, J.M.; Zwart, D.; Lambeck, K.; Wohlfarth, B. Tropical tales of polar ice: Evidence of Last Interglacial polar ice sheet retreat recorded by fossil reefs of the granitic Seychelles islands. *Quat. Sci. Rev.* **2015**, *107*, 182–196. [[CrossRef](#)]
52. Dutton, A.; Rubin, K.; McLean, N.; Bowring, J.; Bard, E.; Edwards, R.; Henderson, G.; Reid, M.; Richards, D.; Sims, K.; et al. Data reporting standards for publication of U-series data for geochronology and timescale assessment in the earth sciences. *Quat. Geochronol.* **2017**, *39*, 142–149. [[CrossRef](#)]
53. Eisele, M.H. The Long-Term Development of Cold-Water Coral Mounds in the NE-Atlantic. Ph.D. Thesis, University of Bremen, Bremen, Germany, 2010.
54. Eisenhauer, A.; Wasserburg, G.; Chen, J.; Bonani, G.; Collins, L.; Zhu, Z.; Wyrwoll, K. Holocene sea-level determination relative to the Australian continent: U/Th (TIMS) and  $^{14}\text{C}$  (AMS) dating of coral cores from the Abrolhos Islands. *Earth Planet. Sci. Lett.* **1993**, *114*, 529–547. [[CrossRef](#)]
55. Esat, T.M.; McCulloch, M.T.; Chappell, J.; Pillans, B.; Omura, A. Rapid Fluctuations in Sea Level Recorded at Huon Peninsula During the Penultimate Deglaciation. *Science* **1999**, *283*, 197–201. [[CrossRef](#)]
56. Esat, T.; Yokoyama, Y. Variability in the uranium isotopic composition of the oceans over glacial–interglacial timescales. *Geochim. Cosmochim. Acta* **2006**, *70*, 4140–4150. [[CrossRef](#)]
57. Hamelin, B.; Bard, E.; Zindler, A.; Fairbanks, R.G.  $^{234}\text{U}/^{238}\text{U}$  mass spectrometry of corals: How accurate is the U-Th age of the last interglacial period? *Earth Planet. Sci. Lett.* **1991**, *106*, 169–180. [[CrossRef](#)]
58. Gallup, C.D.; Edwards, R.L.; Johnson, R.G. The timing of high sea levels over the past 200,000 years. *Science* **1994**, *263*, 796–800. [[CrossRef](#)]
59. Gutjahr, M.; Vance, D.; Hoffmann, D.L.; Hillenbrand, C.-D.; Foster, G.; Rae, J.; Kuhn, G. Structural limitations in deriving accurate U-series ages from calcitic cold-water corals contrast with robust coral radiocarbon and Mg/Ca systematics. *Chem. Geol.* **2013**, *355*, 69–87. [[CrossRef](#)]
60. Correa, M.L.; Montagna, P.; Joseph, N.; Rüggeberg, A.; Fietzke, J.; Flögel, S.; Dorschel, B.; Goldstein, S.; Wheeler, A.; Freiwald, A. Preboreal onset of cold-water coral growth beyond the Arctic Circle revealed by coupled radiocarbon and U-series dating and neodymium isotopes. *Quat. Sci. Rev.* **2012**, *34*, 24–43. [[CrossRef](#)]
61. Ludwig, K.R.; Szabo, B.J.; Moore, J.G.; Simmons, K.R. Crustal subsidence rate off Hawaii determined from  $^{234}\text{U}/^{238}\text{U}$  ages of drowned coral reefs. *Geology* **1991**, *19*, 171–174. [[CrossRef](#)]
62. Ludwig, K.R.; Muhs, D.R.; Simmons, K.R.; Halley, R.B.; Shinn, E.A. Sea-level records at ~80 ka from tectonically stable platforms: Florida and Bermuda. *Geology* **1996**, *24*, 211–214. [[CrossRef](#)]
63. Muhs, D.R.; Simmons, K.R.; Steinke, B. Timing and warmth of the Last Interglacial period: New U-series evidence from Hawaii and Bermuda and a new fossil compilation for North America. *Quat. Sci. Rev.* **2002**, *21*, 1355–1383. [[CrossRef](#)]
64. Potter, E.-K.; Esat, T.; Schellmann, G.; Radtke, U.; Lambeck, K.; McCulloch, M. Suborbital-period sea-level oscillations during marine isotope substages 5a and 5c. *Earth Planet. Sci. Lett.* **2004**, *225*, 191–204. [[CrossRef](#)]
65. Potter, E.-K.; Stirling, C.H.; Wiechert, U.H.; Halliday, A.N.; Spötl, C. Uranium-series dating of corals in situ using laser-ablation MC-ICPMS. *Int. J. Mass Spectrom.* **2005**, *240*, 27–35. [[CrossRef](#)]
66. Roberts, G.P.; Houghton, S.L.; Underwood, C.; Papanikolaou, I.; Cowie, P.A.; Van Calsteren, P.; Wigley, T.; Cooper, F.J.; McArthur, J.M. Localization of Quaternary slip rates in an active rift in 105 years: An example from central Greece constrained by  $^{234}\text{U}$ – $^{230}\text{Th}$  coral dates from uplifted paleoshorelines. *J. Geophys. Res. Space Phys.* **2009**, *114*, B1046. [[CrossRef](#)]
67. Shaked, Y.; Agnon, A.; Lazar, B.; Marco, S.; Avner, U.; Stein, M. Large earthquakes kill coral reefs at the north-west Gulf of Aqaba. *Terra Nova* **2004**, *16*, 133–138. [[CrossRef](#)]
68. Shen, C.-C.; Li, K.-S.; Sieh, K.; Natawidjaja, D.; Cheng, H.; Wang, X.; Edwards, R.L.; Lam, D.D.; Hsieh, Y.-T.; Fan, T.-Y.; et al. Variation of initial  $^{230}\text{Th}/^{232}\text{Th}$  and limits of high precision U–Th dating of shallow-water corals. *Geochim. Cosmochim. Acta* **2008**, *72*, 4201–4223. [[CrossRef](#)]
69. Stein, M.; Wasserburg, G.; Aharon, P.; Chen, J.; Zhu, Z.; Bloom, A.; Chappell, J. TIMS U-series dating and stable isotopes of the last interglacial event in Papua New Guinea. *Geochim. Cosmochim. Acta* **1993**, *57*, 2541–2554. [[CrossRef](#)]

70. Stirling, C.; Esat, T.; Lambeck, K.; McCulloch, M. Timing and duration of the Last Interglacial: Evidence for a restricted interval of widespread coral reef growth. *Earth Planet. Sci. Lett.* **1998**, *160*, 745–762. [[CrossRef](#)]
71. Thomas, A.L.; Fujita, K.; Iryu, Y.; Bard, E.; Cabioch, G.; Camoin, G.; Cole, J.E.; Deschamps, P.; Durand, N.; Hamelin, B.; et al. Assessing subsidence rates and paleo water-depths for Tahiti reefs using U-Th chronology of altered corals. *Mar. Geol.* **2012**, *295–298*, 86–94. [[CrossRef](#)]
72. Thompson, W.G.; Spiegelman, M.W.; Goldstein, S.L.; Speed, R.C. An open-system model for U-series age determinations of fossil corals. *Earth Planet. Sci. Lett.* **2003**, *210*, 365–381. [[CrossRef](#)]
73. Yokoyama, Y.; Esat, T.M. Long term variations of uranium isotopes and radiocarbon in the surface seawater recorded in corals. In *Global Environmental Change in the Ocean and on Land*; Shiyomi, M., Kawahata, H., Koizumi, H., Tsuda, A., Awaya, Y., Eds.; TERRAPUB: Tokyo, Japan, 2004; pp. 279–309.
74. Yokoyama, Y.; Esat, T.; Lambeck, K. Coupled climate and sea-level changes deduced from Huon Peninsula coral terraces of the last ice age. *Earth Planet. Sci. Lett.* **2001**, *193*, 579–587. [[CrossRef](#)]
75. Spratt, R.M.; Lisiecki, L.E. A Late Pleistocene sea level stack. *Clim. Past.* **2016**, *12*, 1079–1092. [[CrossRef](#)]
76. Zykov, S.B.; Kiselev, G.P.; Zykova, E.N. New data on the uranium-isotopic composition of the Barents Sea water. In *Radioactivity and Radioactive Elements in the Human Environment*; Rikhvanov, L.P., Ed.; Tomsk State University: Tomsk, Tussai, 2013; pp. 214–217.
77. Scholten, J.; Botz, R.; Paetsch, H.; Stoffers, P.; Weinelt, M. High-resolution uranium-series dating of Norwegian-Greenland Sea sediments: 230Th vs.  $\delta^{18}O$  stratigraphy. *Mar. Geol.* **1994**, *121*, 77–85. [[CrossRef](#)]
78. Bezrukova, E.V. *Paleogeography of the Baikal Region in the Late Glacial and Holocene*; Nauka: Novosibirsk, Russia, 1999.
79. Biskaborn, B.K.; Smith, S.L.; Noetzli, J.; Matthes, H.; Vieira, G.; Streletskiy, D.A.; Schoeneich, P.; Romanovsky, V.E.; Lewkowicz, A.G.; Abramov, A.; et al. Permafrost is warming at a global scale. *Nat. Commun.* **2019**, *10*, 264. [[CrossRef](#)]
80. Afanasiev, A.H. *Water Resources and Water Balance of the Lake Baikal*; Nauka: Novosibirsk, Russia, 1976.
81. Karabanov, E.B.; Prokopenko, A.A.; Kuzmin, M.I.; Williams, D.F.; Gvozdkov, A.N.; Kerber, E.V. Glaciation and interglacials of Siberia—Paleoclimatic record from Lake Baikal and its correlation with the West Siberian stratigraphy (Brunhes era of direct polarity). *Russ. Geol. Geophys.* **2001**, *42*, 48–63.
82. Kuzmin, M.I.; Bychinsky, V.A.; Kerber, E.V.; Oshchepkova, A.V.; Goreglyad, A.V.; Ivanov, E.V. Chemical composition of sediments of deep-water Baikal wells as a basis for reconstruction of climate and environmental changes. *Russ. Geol. Geophys.* **2014**, *55*, 3–22.
83. Stolpovskaya, V.N.; Solotchina, E.P.; Zhdanova, A.N. Quantitative IR spectroscopic analysis of non-clay minerals from the bottom sediments of Lakes Baikal and Hovsgol (in the context of paleoclimatic reconstructions). *Russ. Geol. Geophys.* **2006**, *47*, 778–788.
84. Chebykin, E.P. Express Mass Spectrometric Determination of Elements and Natural Isotopes of Uranium and Thorium in Sediments of Lake Baikal for Their Dating and Deciphering of Paleoclimate Parameters. Ph.D. Thesis, Limnological Institute, Irkutsk, Russia, 2006.
85. Chebykin, E.; Goldberg, E.; Kulikova, N. Elemental composition of suspended particles from the surface waters of Lake Baikal in the zone affected by the Selenga River. *Russ. Geol. Geophys.* **2010**, *51*, 1126–1132. [[CrossRef](#)]
86. Carter, S.J.; Colman, S.M. Biogenic silica in Lake Baikal sediments: Results from 1990–1992 American cores. *J. Great Lakes Res.* **1994**, *20*, 751–760. [[CrossRef](#)]
87. Colman, S.M.; Jones, G.A.; Rubin, M.; King, J.W.; Peck, J.A.; Orem, W.H. AMS radiocarbon analyses from Lake Baikal, Siberia: Challenges of dating sediments from a large, oligotrophic lake. *Quat. Sci. Rev.* **1996**, *15*, 669–684. [[CrossRef](#)]
88. Chebykin, E.P.; Edgington, D.N.; Grachev, M.A.; Zheleznyakova, T.O.; Vorobyova, S.S.; Kulikova, N.S.; Azarova, I.N.; Khlystov, O.M.; Goldberg, E.L. Abrupt increase in precipitation and weathering of soils in East Siberia coincident with the end of the last glaciation (15 cal kyr BP). *Earth Planet. Sci. Lett.* **2002**, *200*, 167–175. [[CrossRef](#)]
89. Demory, F.; Oberhänsli, H.; Nowaczyk, N.R.; Gottschalk, M.; Wirth, R.; Naumann, R. Detrital input and early diagenesis in sediments from Lake Baikal revealed by rock magnetism. *Glob. Planet. Chang.* **2005**, *46*, 145–166. [[CrossRef](#)]
90. Edgington, D.; Robbins, J.; Colman, S.; Orlandini, K.; Gustin, M.-P. Uranium-series disequilibrium, sedimentation, diatom frustules, and paleoclimate change in Lake Baikal. *Earth Planet. Sci. Lett.* **1996**, *142*, 29–42. [[CrossRef](#)]
91. Fagel, N.; Thamó-Bózsó, E.; Heim, B. Mineralogical signatures of Lake Baikal sediments: Sources of sediment supplies through Late Quaternary. *Sediment. Geol.* **2007**, *194*, 37–59. [[CrossRef](#)]
92. Goldberg, E.; Phedorin, M.; Grachev, M.; Bobrov, V.; Dolbnya, I.; Khlystov, O.; Levina, O.; Ziborova, G. Geochemical signals of orbital forcing in the records of paleoclimates found in the sediments of Lake Baikal. *Nucl. Instrum. Methods Phys. Res. Sect. A Accel. Spectrometers Detect. Assoc. Equip.* **2000**, *448*, 384–393. [[CrossRef](#)]
93. Goldberg, E.; Grachev, M.; Chebykin, E.; Phedorin, M.; Kalugin, I.; Khlystov, O.; Zolotarev, K. Scanning SRXF analysis and isotopes of uranium series from bottom sediments of Siberian lakes for high-resolution climate reconstructions. *Nucl. Instrum. Methods Phys. Res. Sect. A Accel. Spectrometers Detect. Assoc. Equip.* **2005**, *543*, 250–254. [[CrossRef](#)]
94. Goldberg, E.; Chebykin, E.; Zhuchenko, N.; Vorobyeva, S.S.; Stepanova, O.; Khlystov, O.; Ivanov, E.; Weinberg, E.; Gvozdkov, A. Uranium isotopes as proxies of the environmental history of the Lake Baikal watershed (East Siberia) during the past 150ka. *Palaeogeogr. Palaeoclim. Palaeoecol.* **2010**, *294*, 16–29. [[CrossRef](#)]
95. Grachev, M.A.; Vorobyova, S.S.; Likhoshway, E.V.; Goldberg, E.L.; Ziborova, G.A.; Levina, O.V.; Khlystov, O.M. A high resolution diatom record of the palaeoclimates of East Siberia for the last 2.5 my from Lake Baikal. *Quat. Sci. Rev.* **1998**, *17*, 1101–1106. [[CrossRef](#)]

96. Horiuchi, K.; Minoura, K.; Hoshino, K.; Oda, B.; Nakamura, T.; Kawai, T. Palaeoenvironmental history of Lake Baikal during the last 23000 years. *Palaeogeogr. Palaeoclimatol. Palaeoecol.* **2000**, *157*, 95–108. [[CrossRef](#)]
97. Kashiwaya, K. *Long Continental Records from Lake Baikal*; Springer: Tokyo, Japan, 2003.
98. Khursevich, G.K.; Karabanov, E.B.; Prokopenko, A.A.; Williams, D.F.; Kuzmin, M.I.; Fedenya, S.A.; Gvozdkov, A.A. Insolation regime in Siberia as a major factor controlling diatom production in Lake Baikal during the past 800,000 years. *Quat. Int.* **2001**, *80–81*, 47–58. [[CrossRef](#)]
99. Kuzmin, M.I.; Karabanov, E.B.; Kawai, T.; Williams, D.; Bychinsky, V.A.; Kerber, E.V.; Kravchinsky, V.A.; Bezrukova, E.V.; Prokopenko, A.A.; Geletti, V.F.; et al. Deep drilling on Lake Baikal: Main results. *Russ. Geol. Geoph.* **2001**, *42*, 3–28.
100. Morgenstern, U.; Ditchburn, R.G.; Vologina, E.G.; Sturm, M. <sup>32</sup>Si dating of sediments from Lake Baikal. *J. Paleolimnol.* **2013**, *50*, 345–352. [[CrossRef](#)]
101. Och, L.M.; Müller, B.; Wichser, A.; Ulrich, A.; Vologina, E.G.; Sturm, M. Rare earth elements in the sediments of Lake Baikal. *Chem. Geol.* **2014**, *376*, 61–75. [[CrossRef](#)]
102. Prokopenko, A.A.; Karabanov, E.B.; Williams, D.F.; Kuzmin, M.I.; Shackleton, N.J.; Crowhurst, S.J.; Peck, J.A.; Gvozdkov, A.N.; King, J.W. Biogenic Silica Record of the Lake Baikal Response to Climatic Forcing during the Brunhes. *Quat. Res.* **2001**, *55*, 123–132. [[CrossRef](#)]
103. Shchetnikov, A.A.; Bezrukova, E.V.; Maksimov, F.E.; Kuznetsov, V.Y.; Filinov, I.A. Environmental and climate reconstructions of the Fore-Baikal area during MIS 5-1: Multiproxy record from terrestrial sediments of the Ust-Oda section (Siberia, Russia). *J. Asian Earth Sci.* **2016**, *129*, 220–230. [[CrossRef](#)]
104. Sklyarova, O.; Sklyarov, E.; Och, L.; Pastukhov, M.; Zagorulko, N. Rare earth elements in tributaries of Lake Baikal (Siberia, Russia). *Appl. Geochem.* **2017**, *82*, 164–176. [[CrossRef](#)]
105. Sturm, M.; Vologina, E.G.; Vorob'Eva, S.S. Holocene and Late Glacial sedimentation near steep slopes in southern Lake Baikal. *J. Limnol.* **2016**, *75*, 24–35. [[CrossRef](#)]
106. Tarasov, P.; Bezrukova, E.; Karabanov, E.; Nakagawa, T.; Wagner, M.; Kulagina, N.; Letunova, P.; Abzaeva, A.; Granoszewski, W.; Riedel, F. Vegetation and climate dynamics during the Holocene and Eemian interglacials derived from Lake Baikal pollen records. *Palaeogeogr. Palaeoclim. Palaeoecol.* **2007**, *252*, 440–457. [[CrossRef](#)]
107. Tyszkowski, S.; Kaczmarek, H.; Słowiński, M.; Kozyreva, E.; Brykała, D.; Rybchenko, A.; Babicheva, V. Geology, permafrost, and lake level changes as factors initiating landslides on Olkhon Island (Lake Baikal, Siberia). *Landslides* **2014**, *12*, 573–583. [[CrossRef](#)]
108. Watanabe, T.; Nakamura, T.; Nara, F.W.; Kakegawa, T.; Horiuchi, K.; Senda, R.; Oda, T.; Nishimura, M.; Matsumoto, G.I.; Kawai, T. High-time resolution AMS <sup>14</sup>C data sets for Lake Baikal and Lake Hovsgol sediment cores: Changes in radiocarbon age and sedimentation rates during the transition from the last glacial to the Holocene. *Quat. Int.* **2009**, *205*, 12–20. [[CrossRef](#)]
109. Fleisher, R.L.; Raabe, O.G. Recoiling alpha-emitting nuclei. Mechanisms for uranium-series disequilibrium. *Geochim. Cosmochim. Acta* **1978**, *42*, 973–978. [[CrossRef](#)]
110. Hovsgol Drilling Project (HDP) Members. Sedimentary record from Lake Hovsgol, NW Mongolia: Results from the HDP-04 and HDP-06 drill cores. *Quat. Int.* **2009**, *205*, 21–37. [[CrossRef](#)]
111. Katsuta, N.; Matsumoto, G.I.; Tani, Y.; Tani, E.; Murakami, T.; Kawakami, S.-I.; Nakamura, T.; Takano, M.; Matsumoto, E.; Abe, O.; et al. A higher moisture level in the early Holocene in northern Mongolia as evidenced from sediment records of Lake Hovsgol and Lake Erhel. *Quat. Int.* **2017**, *455*, 70–81. [[CrossRef](#)]
112. Kim, B.; Cheong, D.; Lee, E. Palaeoenvironmental changes in northern Mongolia during the last deglaciation revealed by trace element records in ostracods from Lake Hovsgol. *Quat. Int.* **2015**, *384*, 169–179. [[CrossRef](#)]
113. Mochizukia, A.; Murata, T.; Hosoda, K.; Katano, T.; Tanaka, Y.; Mimura, T.; Mitamura, O.; Nakano, S.; Okazaki, Y.; Sugiyama, Y.; et al. Distributions and geochemical behaviors of oxyanion-forming trace elements and uranium in the Hövsgöl-Baikal-Yenisei water system of Mongolia and Russia. *J. Geochem. Explor.* **2018**, *188*, 123–136. [[CrossRef](#)]
114. Orkhonselenge, A.; Krivonogov, S.K.; Mino, K.; Kashiwaya, K.; Safonova, I.Y.; Yamamoto, M.; Kashima, K.; Nakamura, T.; Kim, J.Y. Holocene sedimentary records from Lake Borsog at the eastern shore of Lake Hovsgol, Mongolia, and their palaeoenvironmental implications. *Quat. Int.* **2013**, *290–291*, 95–109. [[CrossRef](#)]
115. Oyunchimeg, T.; Chebykin, E.P. High-Performance Technique on the Base of ICP-MS for Obtaining High-Resolution Records of Climate-Sensitive Elements in Bottom Sediments of Lake Hovsgol (Mongolia). *Chem. Sustain. Dev.* **2009**, *17*, 97–110.
116. Prokopenko, A.A.; Khursevich, G.K.; Bezrukova, E.V.; Kuzmin, M.I.; Boes, X.; Williams, D.F.; Fedenya, S.A.; Kulagina, N.V.; Letunova, P.P.; Abzaeva, A.A. Palaeoenvironmental proxy records from Lake Hovsgol, Mongolia, and a Synthesis of Holocene Climate Change in the Lake Baikal watershed. *Quat. Res.* **2007**, *68*, 2–17. [[CrossRef](#)]
117. Solotchina, E.P.; Prokopenko, A.A.; Kuzmin, M.I.; Solotchin, P.A.; Zhdanova, A.N. Climate signals in sediment mineralogy of Lake Baikal and Lake Hovsgol during the LGM-Holocene transition and the 1-Ma carbonate record from the HDP-04 drill core. *Quat. Int.* **2009**, *205*, 38–52. [[CrossRef](#)]
118. Watanabe, T.; Minoura, K.; Nara, F.W.; Shichi, K.; Horiuchi, K.; Kakegawa, T.; Kawai, T. Last glacial to post glacial climate changes in continental Asia inferred from multi-proxy records (geochemistry, clay mineralogy, and paleontology) from Lake Hovsgol, northwest Mongolia. *Glob. Planet. Chang.* **2012**, *88–89*, 53–63. [[CrossRef](#)]
119. Zhang, C.; Zhang, W.; Feng, Z.; Mischke, S.; Gao, X.; Gao, D.; Sun, F. Holocene hydrological and climatic change on the northern Mongolian Plateau based on multi-proxy records from Lake Gun Nuur. *Palaeogeogr. Palaeoclim. Palaeoecol.* **2012**, *323–325*, 75–86. [[CrossRef](#)]

120. Vosel, Y.S. Geochemistry of Uranium in Modern Carbonate Deposits of Small Lakes: Forms of Occurrence and Isotopic Ratios  $^{234}\text{U}/^{238}\text{U}$ . Ph.D. Thesis, Novosibirsk State University, Novosibirsk, Russia, 2015.
121. Chebykin, E.P.; Sorokovikova, L.M.; Tomberg, I.V.; Vodneva, E.N.; Rasskazov, S.V.; Khodzher, T.V.; Grachev, M.A. Current state of the river. Selenga on the territory of Russia by main components and trace elements. *Chem. Sustain. Dev.* **2012**, *20*, 613–631.
122. Rasskazov, S.V.; Chebykin, E.P.; Ilyasova, A.M.; Vodneva, E.N.; Chuvashova, I.S.; Bornyakov, S.A.; Seminsky, A.K.; Snopkov, S.V.; Chechel'nitsky, V.V.; Gileva, N.A. Creating the Kultuk polygon for earthquake prediction: Variations of ( $^{234}\text{U}/^{238}\text{U}$ ) and  $^{87}\text{Sr}/^{86}\text{Sr}$  in groundwater from active faults at the western shore of Lake Baikal. *Geodyn. Tectonophys.* **2015**, *26*, 519–554. [[CrossRef](#)]